ISBN: 978-3-95450-204-2 ISSN: 2673-5350 doi:10.18429/JACoW-IBIC2019-MOPP022

NEUTRON SENSITIVE BEAM LOSS MONITORING SYSTEM FOR THE ESS LINAC

I. Dolenc Kittelmann*, F. S. Alves, E. Bergman, C. Derrez, V. Grishin,
K. Rosengren, T. J. Shea, ESS ERIC, Lund, Sweden
Q. Bertrand, T. Joannem, P. Legou, Y. Mariette, V. Nadot, T. Papaevangelou,
L. Segui, IRFU, CEA, Gif-sur-Yvette, France
W. Cichalewski, G. W. Jabłoński, W. Jałmużna, R. Kiełbik, TUL, DMCS, Łódź, Poland

Abstract

The European Spallation Source (ESS), currently under construction in Lund, Sweden, will be a neutron source based on partly superconducting linac, accelerating protons to 2 GeV with a peak current of 62.5 mA, ultimately delivering a 5 MW beam to a rotating tungsten target. For a successful tuning and operation of a linac, a Beam Loss Monitoring (BLM) system is required. The system is designed to protect the machine from beam-induced damage and unnecessary activation of the components. This contribution focuses on one of the BLM systems to be deployed at the ESS linac, namely the neutron sensitive BLM (nBLM). Recently, test of the nBLM data acquisition chain including the detector has been performed at LINAC4, at CERN. The test represents first evaluation of the system prototype in realistic environment. Results of the test will be presented together with an overview of the ESS nBLM system.

INTRODUCTION

The European Spallation Source (ESS) is a material science facility, which is currently being built in Lund, Sweden and will provide neutron beams for neutron-based research [1]. The neutron production will be based on bombardment of a tungsten target with a proton beam of 5 MW average power. A linear accelerator (linac) will accelerate protons up to 2 GeV and transport them towards the target through a sequence of a normal conducting (NC) and superconducting (SC) accelerating structures (Fig. 1).

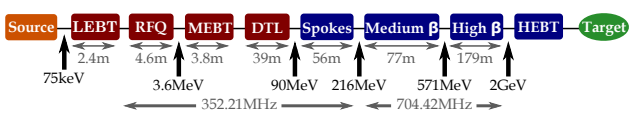

Figure 1: The ESS linac layout [1]. Red colour represents the NC and blue the SC parts of the linac.

As in case of all future high-power accelerators, ESS linac operation will be limited by beam losses if machine activation is to be kept low enough for hands-on maintenance. Moreover, loss of even a small fraction of intense ESS beam can result in a significant increase of irradiation levels, ultimately leading to damage of the linac components. Beam Loss Monitoring (BLM) systems are designed to provide information about beam loss levels. Thus, they play an important role in machine fine tuning as well as machine protection from beam-induced damage by detecting unacceptably high beam losses and promptly inhibiting beam production.

Two types of BLM systems differing in detector technology have been conceived at ESS. The neutron sensitive BLM (nBLM) system is based on 82 neutron detectors primarily covering the lower energy part of the ESS linac. Conversely, the Ionisation Chamber based BLM (ICBLM) system consists of 266 ionisation chambers located almost exclusively throughout the SC parts of the linac [2].

This contribution aims to report an overview of the nBLM system design. In addition to this, results of the test performed with the first prototype in realistic environment are presented.

DETECTOR DESIGN

The nBLM system is based on neutron-sensitive Micromegas devices [3], specially designed to primarily cover the lower energy part of the ESS linac. Monte Carlo simulation studies were used to optimise the detector design and locations in order to assure coverage and redundancy for the machine protection purposes and provide spatial resolution for the diagnostic purposes [4, 5].

One of the challenges when measuring beam losses in a linac is related to the RF-induced background. This background is mainly due to the electron field emission from RF cavity walls resulting in bremsstrahlung photons created on the cavity or beam pipe materials [6]. For this reason, the nBLM detectors are designed to be sensitive to fast neutrons and exhibit low sensitivity to low-energy photons. Additionally, the signals due to thermal neutrons are suppressed as they may not be directly correlated to the beam losses. This is achieved by equipping the detector with suitable absorber and neutron converter materials.

Two types of nBLM detectors with complementary functionality have been developed. Fast detectors (nBLM-F) aim to detect fast losses when high particle fluxes due to accidental beam losses are expected. On the other hand, slow detectors (nBLM-S) primarily aim to monitor slow losses when low particle fluxes are expected. Details of the final detector module design and performance are available at this conference in a separate contribution [7].

Time characteristics of nBLM-F and nBLM-S signal pulses are the same, however neutron moderation in case of nBLM-S delays a big part of events by amount of time ranging from tens of ns to ~200 µs. A typical signal pro-

* irena.dolenckittelmann@esss.se

ISBN: 978-3-95450-204-2 ISSN: 2673-5350 doi:10.18429/JACoW-IBIC2019-MOPP022

duced by an incoming particle in these detectors is a negative pulse with a rise time of 30–50 ns and pulse duration of 100–200 ns, depending on the applied electric fields in the detector chamber.

COVERAGE AND DETECTOR LAYOUT

Following the goal of nBLM system as the primary loss monitor in the NC parts of the ESS linac, the majority of detectors will be placed in the DTL section (Fig. 1). Here detectors will be positioned at every ~ 1/4 (~1 m) of a DTL tank length, resulting in 8 detectors per each tank and a pair at the end of the DTL section. The placement is consistent with Monte Carlo simulation results where standard deviation of secondary neutron distributions 20 cm away from the tanks was found to vary between 0.9–3.6 m for a set of point loss scenarios in DTL differing in beam parameters.

A significant number of detectors will be located in the Spoke section following the DTL in order to smooth the transition in coverage between nBLM as the primary monitor in the NC linac and ICBLM in the SC linac. The arrangement also allows an option to compare the measurements between the two systems to potentially better understand the background signal. Other high energy parts of the linac are only sparsely populated with nBLM detectors.

Majority of the nBLM detectors will be placed in an alternating fashion by varying between nBLM-F and -S type along the linac (Fig. 2). Though at certain position a pair of both will be located. Alternating between the types will be present in the DTL with the exception of a detector pair at the end. The same holds for the Spoke section where one slow and one fast detector will be placed at each cryomodule and the region between two successive cryomodules, respectively. In other SC parts of the linac a pair of slow and fast detectors will be placed at few locations along the linac, while two detector pairs will be present in the MEBT.

SYSTEM ARCHITECTURE

Each detector is enclosed in a detector module together with the custom Front End Electronics (FEE). Analogue signals are routed from detector modules in the linac tunnel to the Back End Electronics (BEE) racks in the Klystron Gallery. Here, the signal is first digitised and sampled at 250 MS/s rate by a DC-coupled, 8-channel, 16-bit ADC (IOxOS ADC3111 FMC [8]). The signal is then processed in real time by MTCA.4–based AMC board (IOxOS IFC1410 [9]) equipped with Xilinx Kintex Ultrascale FPGA. The board handles up to 6 detector channels simultaneously and manages the communication to the Machine Protection System (MPS). Monitoring and control of the system (including data acquisition and slow control) is managed through an EPICS based software, running on the CPUs located in the MTCA crates.

Two CAEN SY4527 [10] crates will be used to control high (HV) and low (LV) voltage power supplies. The 48-channel module CAEN A7030 [11] will bias the detectors, while the 8-channel CAEN A2519 [12] will power the FEE, where one LV channel is used per group of up to 6 detectors.

In order to increase system robustness and to avoid situations when a certain electronics failure results in the system being unable to react on dangerous beam conditions, the detectors are grouped in three groups with respect to electronics layout. The first two groups cover linac parts up to including Spoke section containing majority of nBLM detectors. They are formed by collecting odd and even pairs of neighbouring fast and slow detectors. The groups have all signal connections in separate racks, so that no odd group detector connects to a rack reserved for even detectors and vice versa. The third group covers the rest of the detectors in the high energy parts. The longest signal cable length of this layout is estimated to be below 100 m.

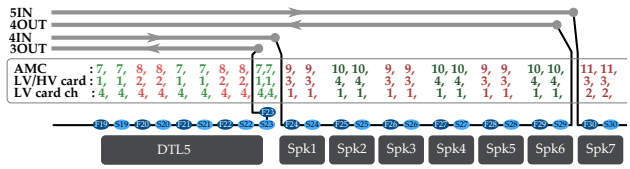

Figure 2: Detector and electronics layout in DTL tank 5 and initial 7 subsections of the Spoke section. See text for explanation.

Both HV and LV connections follow the same detector grouping as the signal connections. However, with limited number of HV/LV crates, the separation between odd and even groups is possible only to the HV/LV card level. Here a set of detectors with signal cables connected to certain AMC card has FEE powered by the same LV channel. Similarly, a set of detectors with signal connections to a certain rack has the HV/LV cables connected to the same HV/LV module.

The idea of HV/LV and signal connections is schematically presented in Fig. 2 for part of the linac. Here odd and even detector groups are indicated by green and red colour, respectively. Numbers in rows marked as “AMC”, “LV/HV card” and “LV card ch” correspond to AMC card ID, LV/HV card ID and LV card channel the detectors (positioned below numbers) connect to. The detectors are indicated with blue, where F stands for nBLM-F and S for nBLM-S. Gray and black lines represent long haul and short gas tubes.

Micromegas devices are gaseous detectors that require a continuous gas flow (1–2 L/h) to insure stable operation on a time scale of years. Thus, the nBLM system is designed to work in a circulation mode. The gas mixture used consists of He and 10 % CO_2. One distribution and one return stainless steel gas line are routed from the bottles with premixed gas, located in the storage placed outside, to a dedicated rack inside the Klystron Gallery. The rack houses one main and two distribution crates to control the gas flow. Here both distribution and return lines are split in 6 long haul lines which are further routed to the accelerator tunnel. The 12 lines end at different points along the linac where they are continued with polyurethane tubes to form 6 loops. Each of these loops circulates gas through a group of 10–20 neighbouring detectors connected with polyurethane tubes in series.

ISBN: 978-3-95450-204-2 ISSN: 2673-5350 doi:10.18429/JACoW-IBIC2019-MOPP022

DATA PROCESSING

Monte Carlo simulations [5] show that at higher loss levels, the nBLM system can experience pileup of neutron events and eventually transition from single event counting to current mode of operation. The transition is performed automatically by the FPGA based real-time data processing as given below.

The main task of a BLM system is to detect beam instabilities that might cause damage to the linac equipment. When such conditions are detected, the system triggers a stop of beam production by dropping the BEAM_PERMIT signal which is continuously transmitted to the Beam Interlock System (BIS), the backbone of the MPS. Additionally the system provides information about the beam losses for monitoring purposes in order to avoid unnecessary activation of the linac equipment.

This is achieved by continuous processing of the digitised incoming raw signal from each nBLM detector in order to provide N_n, the number of detected neutrons per Monitoring Time Window (MTW), which relates to the beam loss. The length of MTW was set to 1 µs in order to comply with the 5 µs response time requirement of the system for machine protection purposes and time characteristics of the signal pulse produced by an incoming single neutron.

At the beginning of the processing chain, a fixed detector-dependent pedestal value is subtracted form each raw data sample. The processing is continued with the Neutron Detection Algorithm (NDA) primarily providing N_n every µs.

NDA starts by first identifying Interesting Events (IEs). An IE is considered to start whenever the signal falls below a certain event detection threshold (S_{EDT}) and end when signal raises back above this value (Fig. 3). For each IE certain pulse characteristics (amplitude A, Time-Over-Threshold TOT, event charge Q_{TOT}, etc) are extracted and stored in a so called EventInfo structure.

IEs can be classified as neutron or non-neutron events based on their origin. Furthermore, a neutron event can either be due to a single neutron or several neutrons. The latter occurs when the rate of incoming neutrons is too high for the system to distinguish between two single neutron events leading to event pileup. Non-neutron events are caused by noise spikes or background particles (mostly X– and γ-rays) with their rate depending on S_{EDT} and environment for given detector operation conditions.

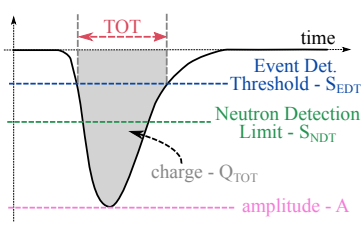

Figure 3: Sketch of a neutron event with NDA settings and some of the pulse characteristics.

The basic idea behind the NDA is to distinguish between single neutron (SNE), pileup (PE) and non-neutron events (NNE) and accordingly extract N_n every MTW. In case of a SNE, N_n is increased by one, while for a PE the number is estimated from the event charge, Q_{TOT} extracted as the integral of the signal over event TOT (see Fig. 3).

An IE is regarded as SNE when event TOT exceeds a certain limit and amplitude A falls below a predefined neutron detection threshold, S_{NDT}. In case TOT of a neutron event is large enough the event is recognised as a PE.

The above description presents a simplified view of the NDA. To improve noise immunity, hysteresis in S_{EDT} is introduced in the IE identification. Furthermore, the need to report neutron counts per unit of time without unnecessary delays complicates the data processing, as one cannot wait for the end of the PE indefinitely. Therefore, certain events are terminated at the MTW edge and need special care.

The N_n values are streamed at 1 MHz to the input of Protection Function Algorithm continuously assessing if conditions to inhibit beam production have been met. Here the data is first passed through configurable filters and then compared to the channel dependent thresholds. The final result is a BEAM_PERMIT signal that is aggregated over all functioning channels on each AMC. The signal is continuously transmitted to the BIS that further handles inhibiting of beam production in case of its absence.

The N_n values together with other NDA outputs are additionally used to compute several statistics called Periodic Data, typically extracted on every machine cycle (14 Hz) for monitoring purposes. An example of such monitoring variable is N_n averaged over full machine cycle. In addition to the Periodic Data, certain types of data originating from various stages of processing are being buffered and can be retrieved on demand (Data On Demand - DoD). This among other includes raw detector signal (250 MHz), EventInfo structure (for each IE) and neutron counts N_n (1 MHz).

As both slow and fast detector exhibit the same time characteristics of the signal, the same algorithms are used in both cases. Details about the firmware implementation can be found in [13].

FIRST PROTOTYPE TEST

In 2018, a nBLM-F pre-series detector module was installed at LINAC4 at CERN, in the section where conditions close to the ones expected in the ESS DTL can be expected. The module was placed close to the beam pipe at the inter-tank region between DTL1 and DTL2 tank, where H^- beam energy reaches ~12 MeV. The aim of this data-taking campaign was to perform first test of the full nBLM DAQ chain including a detector in realistic environment. Additionally, the detector response was assessed through offline analysis of data recorded with an oscilloscope. The data was collected in December 2018 during the LINAC4 commissioning. The results of the data collected with the nBLM DAQ are reported in this paper, while conclusions from the data recorded with the oscilloscope are discussed in [7].

ISBN: 978-3-95450-204-2 ISSN: 2673-5350 doi:10.18429/JACoW-IBIC2019-MOPP022

The nBLM DAQ prototype under test was at early stage of its development with a running NDA and possibility to manually trigger Data On Demand, including raw unprocessed data stream in a time window of up to 2 s. The prototype did not include the Periodic Data monitoring features, but the main processing chain was in the final version.

The aforementioned EventInfo data for each IE were collected in several acquisition runs with duration ranging from 5 min to 8 h. Figure 4 shows distribution of number of IEs over amplitude, extracted from all EventInfo focused runs through an offline analysis. Note that due to the need of splitting certain pulses in the real time processing, reconstruction of recorded events is required in order to extract real pulse characteristics like amplitude, resulting in differences observed at higher amplitudes. The reconstructed distribution exhibits expected shape with the first slope due to noise and second slope due to γ particles primarily induced by the RF. Neutrons are observed to dominate at amplitudes above ~30 mV as demonstrated in Fig. 4. The results are consistent with the results obtained from the oscilloscope data [7].

Distributions of reconstructed IEs over amplitude and time inside the machine cycle period for the LINAC4 (1.2 s) have been extracted for each data run (Fig. 5). The obtained distributions may be used to reveal RF and beam pulse structure, assuming that neutrons and γ particles signify the presence of beam and RF pulse, respectively. However, the prototype did not have synchronisation with the LINAC4 timing system resulting in observed RF and beam pulse lengths longer than expected with longer runs exhibiting larger increase. The effect is attributed to drifts of the ADC clock. In order to correct for this effect, a constant clock drift was assumed and a scan over ADC sampling period was performed for each run separately. The best approximation for the ADC sampling period was extracted as the one giving the sharpest RF pulse edges. Typical value for the optimal clock period was found to be around a factor of 5.6×10^{-6} (5.6 ppm) larger then the nominal 4 ns, giving RF pulse FWHM (Full Width At Half Maximum) and 90 % lengths of ~880 µs and ~840 µs, respectively. The beam pulse length was estimated to be roughly ~150 µs, though partial presence in the first ~100 µs can be observed.

The extracted pulse lengths and shapes for both RF and beam are in agreement with the results obtained from the oscilloscope data [7]. The exact LINAC4 conditions are still under investigations, though current information from CERN experts indicates that LINAC4 RF and beam pulse length were stable at ~880 µs and 150 µs, respectively, throughout the whole period of our data taking. The exception is ~1 h when pulse length was set to 600 µs, which may explain a few extra neutron hits between ~84.5–84.8 ms in Fig. 5.

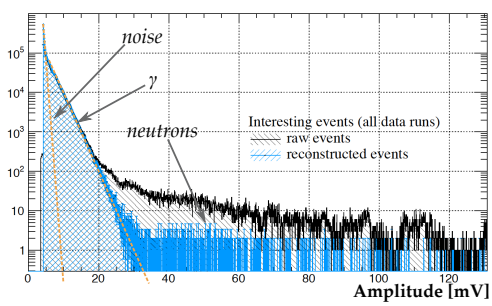

Figure 4: Distribution of number of interesting events over amplitude collected at LINAC4. Blue histogram represents reconstructed data, while black refers to the data as recorded.

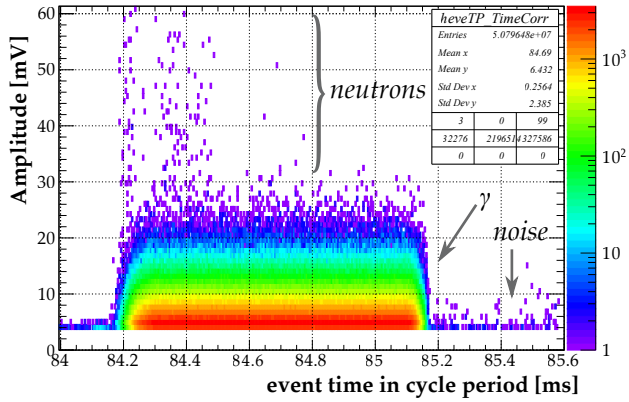

Figure 5: Distribution of reconstructed IEs over amplitude and time inside the LINAC4 machine cycle period for an 8-hour long data run.

SUMMARY AND OUTLOOK

Neutron sensitive BLM system has been developed for the ESS linac. It is based on Micromegas detectors specially designed for the low energy part of the linac. Through real time FPGA based data processing, the system offers the ability to discriminate beam loss induced fast neutrons from both the RF induced photons and background neutrons on event by event basis. In December 2018, the first prototype results have been performed under realistic conditions. The results were found to be in accordance with the oscilloscope data collected separately and discussed in [7]. Part of the system is planned to be installed in the first part of the ESS linac (MEBT and DTL tank 1) by the end of 2019 and commissioned in early 2020.

ACKNOWLEDGEMENTS

The authors would like to thank Christos Zamantzas, Jiří Král and William Viganò for their valuable help with detector installation and realisation of the test at LINAC4.

REFERENCES

[1] R. Garoby *et al.*, "The European Spallation Source Design", *Phys. Scr.*, vol. 93, no. 1, p. 014001, Dec. 2017. doi:10.1088/1402-4896/aa9bff

[2] I. Dolenc Kittelmann *et al.*, "Ionisation Chamber based Beam Loss Monitoring system for the ESS linac", presented at IBIC2019, Malmö, Sweden, Sept. 2019. paper MOPP023.

[3] Y. Giomataris *et al.*, "Development and prospects of the new gaseous detector Micromegas", *Nucl. Instrum. Methods Phys. Res.* A, vol. 419, p. 239–250, Dec. 1998. doi:10.1016/s0168-9002(98)00865-1

ISBN: 978-3-95450-204-2 ISSN: 2673-5350 doi:10.18429/JACoW-IBIC2019-MOPP022

[4] I. Dolenc Kittelmann and T. Shea, "Simulations and detector technologies for the Beam Loss Monitoring System at the ESS linac", in *Proc. HB2016*, Malmö, Sweden, July 2016, paper THAM6Y01, pp. 553–558. doi:10.18429/JACoW-HB2016-THAM6Y01

[5] L. Segui, "Monte Carlo results: nBLM response to ESS scenarios", ESS, Lund, Sweden Rep. ESS-0513010, May, 2017.

[6] J. Norem *et al.*, "The Radiation Environment in and near High Gradient RF Cavities", in *Proc. PAC2001*, Chicago, Illinois, USA, June 2001, paper MPPH030, pp. 837–839.

[7] L. Segui *et al.*, "Characterization and first beam loss detection with one ESS-nBLM system detector", presented at IBIC2019, Malmö, Sweden, Sept. 2019, this conference.

[8] IOxOS ADC3111, https://www.ioxos.ch/produit/adc-3110-3111/

[9] IOxOS IFC1410, https://www.ioxos.ch/produit/ifc_1410/

[10] CAEN SY4527, https://www.caen.it/products/sy4527/

[11] CAEN A7030, https://www.caen.it/products/a7030/

[12] CAEN A2519, https://www.caen.it/products/a2519/

[13] G. Jabłoński *et al.*, "FPGA-based Data Processing in the Neutron-Sensitive Beam Loss Monitoring System for the ESS Linac", presented at MIXDES 2019, Rzeszow, Poland, June 2019, pp. 101–105.